sciendo

DOI: 10.2478/awutp-2020-0003

ANNALS OF WEST UNIVERSITY OF TIMISOARA PHYSICS
Vol. LXII, 2020

ELECTRO-MAGNETIC BEHAVIOR OF HIGHLY CORRELATED FLUORIDES $KFeF_3$, $KCoF_3$ AND $KNiF_3$: A COMPARATIVE *AB-INITIO* STUDY OF CATION EFFECT

Sihem Filalli[1] and Noura Hamdad[2,*]

[1]*Condensed Matter and Sustainable Development Laboratory, Faculty of Sciences, Djillali Liabès University of Sidi Bel-Abbès, Sidi Bel-Abbès 22000, Algeria*
[2]*Faculty of Technology, Djillali Liabès University of Sidi Bel-Abbès, Sidi Bel-Abbès 22000, Algeria*
**Corresponding author: n.hamdad@yahoo.fr*

Article Info

Received: 16.05.2020
Accepted: 01.06.2020

Keywords: Fluorides, DFT, DFT+U, Magnetic moment, and Electronic structure

Abstract

Fluorides-based perovskites are currently the typical materials being used in spintronic devices, optoelectronic and magneto-resistance colossal fields. Solar cells made of Fluoro-perovskite hold much promise for the future of solar energy. The electronic structure and magnetic properties of $KFeF_3$, $KCoF_3$ and $KNiF_3$ Fluorides are studied using ab initio Calculation. We have analysed the structural phases, total and partial electronic densities and band structures within the (DFT) vs the DFT+U description. We show the Electro-Magnetic Behavior using L(S)DA+U vs L(S)DA in a comparative study of cation effect by integrating three types of crystal structures (Cubic (Pm-3m), Four-Layered Hexagonal (P6/mmc), and Orthorhombic (Pnma)). Equilibrium lattices agree very well with experimental and theoretical data. Magnetic moment of each phase is discussed. The obtained results confirmed that the three crystal structures invested here exhibit Ferromagnetic (FM) behavior. The introduction of the Hubbard's parameter U increases lattice parameters and magnetic moment. We deduce that the second cation plays an important role in the magnetic effects. L(S)DA+U show correctly that $KFeF_3$, $KCoF_3$ and $KNiF_3$ are insulators.

1. Introduction

Perovskite originally referred to a mineral calcium titanium oxide, $CaTiO_3$, discovered by Gustav Rose, a German mineralogist and later named after a Russian mineralogist count Lev Aleksevich Perovski. Since then, the ideal cubic phase is investigated in different materials [1-6], with the similar crystal structure and stoichiometry as of $CaTiO_3$, that is, ABX_3, where A is monovalent metallic cation, B is divalent metallic cation, a transition metal and X is a nonmetallic anion (halide). However, for O_2- anions, A and B are divalent and

tetravalent cations, respectively. Recently, intense research on experimental and theoretical fronts have been investigated on perovskite materials (inorganic oxide perovskite and halide perovskite that further encompass alkali halide and organ metal halide perovskite materials, and Fluoro-perovskites named Fluorides if oxygen element is replaced by Fluorine Fe [7-16]. The ideal cubic structure is designated with ABX_3 the B-site cations are similar in size to the X-site anions. While the A-site cations are surrounded by 12 anions in cubo-octahedral coordination, the B-site cations are surrounded by six anions in octahedral coordination. The X-site anions are coordinated by two B-site cations and four A-site cations [17]. They are many alkali metal-divalent metal-fluorides crystallize with perovskite like structures has been known for many years [18]. Fluorides can be considered to have advantages over oxides as their high-pressure phases become stable at much lower pressures [19]. In last decade, many experimental and theoretical investigations have been devoted to the study of perovskite-type fluorides because they have great potential for a variety of device applications in: piezoelectric characteristics [20], ferromagnetic [21], nonmagnetic [22], insulator behavior and photoluminescence [23], optical [24], ferroelectric [25], and antiferromagnetic systems [26−29] due to their wide band gaps. Heterogeneous catalysts [30]. High dielectric permittivity (ε), ferroelectricity, Electronic correlations [31-36] of such 3*d* states are generally strong, they have a more local character and a tendency for insulating states or metal-insulator transitions [37-38], magneto-resistance colossal [39], high capacity memory [40]. As a new generation of promising photovoltaic devices, perovskite solar cells (PSCs) have rapidly evolved in efficiency from 3.8% in 2009 to 23.5% recently [41-43]. Many of researchers have used Ab-Inito calculation to compute as well to predict the electronic structure, elastic, optic, thermal, and magnetic properties of several different classes of perovskite-type 3*d*-transition metal fluorides. The static ab-initio calculations presented here used the projector Full-Potential Linear Augmented Plane waves method embedded in the functional DFT+U description [44, 45] which is One of the mostly implemented methods in the DFT+U realm is the LDA+U method given in the Wien 2K package [46]. The density functional theory (Hohenberg and Kohn 1964 [47], Kohn and Sham 1965 [48]) with the generalized gradient approximation (GGA) PBE pseudopotentials (Perdew et al. 1996) [49] are often used to perform this kind of calculation. We can predict accurately different physical, chemical, mechanical, Thermal, Dielectric, Magnetic properties of the condensed matter even in the absence of theoretical or experimental parameters using these first principles methods. We aim to investigate the electronic energy structure and core-valence states with magnetization effects of $KFeF_3$, $KCoF_3$ and $KNiF_3$ Fluorides by using L(S)DA+U

vs L(S)DA in a comparative study of cation effect by integrating three types of crystal structures (Cubic (Pm-3m), Four-Layered Hexagonal (P6/mmc), and Orthorhombic (Pnma)).

Table1.a: Lattice Cubic (Pm-3m) parameters for $KFeF_3$ Fluoride on the Non-Ferromagnetic (NF) and Ferromagnetic (FM) configurations using different approaches compared with theoretical and experimental work.
i: Ref [101], k: Ref [103], a, b: Ref [105], d: Ref [108], c: Ref [108], and e,: Ref [114].

$KFeF_3$							
Approach	Configuration	a_0(Å)	c_0(Å)	B (GPa)	B'	Vol(Å^3)	Phase
LDA	*Non-Ferromagnetic*	3.863	-	116.41	4.97	57.64	Cubic *Pm-3m*
LDA+U		3.873	-	117.19	4.00	58.09	
L(S)DA	*Ferromagnetic*	4.010	-	93.67	4.37	64.49	
L(S)DA+U		4.033	-	90.89	4.67		
Comparison with theoretical and experimental data							
	Experimental	4.12[a]	-	-	-	-	Cubic *Pm-3m*
	Theoretical	4.061[b]	-	-	-	-	
		4.170 [c]	-	-	-	-	
		4.120[d]	-	-	-	-	
		4.121[e]	-	-	-	-	
		4.122[f]	-	-	-	-	
		4.124 [i]	-	-	-	-	

Table1.b: Lattice 4H-layered Hexagonal (P6/mmc) parameters for $KFeF_3$ Fluoride on the Non-Ferromagnetic (NF) and Ferromagnetic (FM) configurations using different approaches compared with theoretical and experimental work.

Approach	Configuration	a_0(Å)	c_0(Å)	B (GPa)	B'	Vol(Å^3)	Phase
LDA	*Non-Ferromagnetic*	5.499	8.726	109.82	4.49	1658.36	4H-Hexagonal
LDA+U		5.500	8.727	106.86	4.82	1658.72	
L(S)DA	*Ferromagnetic*	5.714	9.067	112.90	1.23	1848.28	
L(S)DA+U		5.727	9.086	87.39	4.20	1872.91	

Table1.c: Lattice Pnma-Orthorhombic parameters for $KFeF_3$ Fluoride on the Non-Ferromagnetic (NF) and Ferromagnetic (FM) configurations using different approaches compared with theoretical and experimental work.

Approach	Configuration	a_0(Å)	c_0(Å)	B (GPa)	B'	Vol(Å^3)	Phase
LDA	*Non-Ferromagnetic*	5.490	7.690	5.398	118.5	4.8	Ortho-rhombic *Pnm*
LDA+U		5.845	8.289	5.483	118.5	4.8	
L(S)DA	*Ferromagnetic*	5.706	7.970	5.591	98.4	4.3	
L(S)DA+U		5.828	8.594	5.691	95.8	4.1	

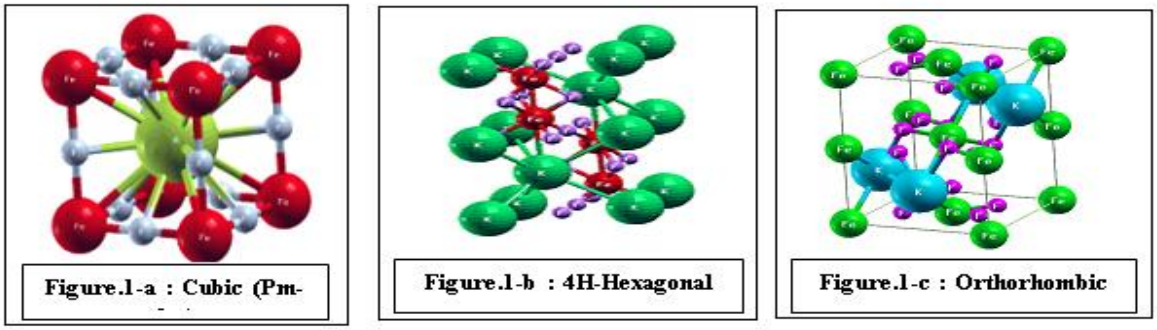

Figure 1. The crystals structures for the $KFeF_3$ Fluoride within (a) Cubic (Pm-3m), (b) 4H- Hexagonal (P63/mmc), and (c) Orthorhombic (Pnma) phases.

2. Theory and Computational Methods

2. A. Crystallographic Model of the Fluoride

For our calculations, we have used the projector Full-Potential Linear Augmented Plane waves method included in the Vienna Ab-initio simulation package. The exchange-correlation potential is taken in consideration by using L(S)DA and L(S)DA+U approaches. Two configurations are invested here Non-Ferromagnetic (NF) and Ferromagnetic (FM) within different crystal phases (Cubic (Pm-3m), 4H-Hexagonal (P6/mmc), and (Pnma) Orthorhombic). According to the literature, it is the tolerance factor that defines the amorphous structure of the Fluoride at a given temperature or pressure. According to the work presented by Tanghong Yi et al. Study [50-52] report that ternary phase Fe(II) fluorides with other alkali metals are known such as K_2FeF_4, $KFeF_3$, and $NaFeF_3$. $KFeF_3$ has a cubic perovskite ABX_3 structure (space group Pm-3m), Jaeryeong Lee et al. shiw [53] have synthesized the reactions proceed with grinding time, and ultimately a single phase of cubic structural $KM_{II}F_3$ (Pm3m) was obtained after grinding for 21.6 ks., V Manivannan et al. [54], Lee et al(2001, 2003) [55-56], synthesized complex metal fluorides with perovskite structures have milled the metal fluorides along with potassium fluorides for 6 h to form KMF_3 (M = Mg, Ca, Zn, Mn, Ni and Co) followed by annealing at 673 K for 2 h to confirm the single-phase formation. The potassium fluoride (KF) and one of alkaline-earth or transition metal

fluoride $M_{II}F_2$. The tolerance factors for $KFeF_3$, $NaFeF_3$, and $LiFeF_3$ (where r_F is substituted for r_O in the equation above) are around 0.91, 0.79, and 0.70, respectively, assuming they all retain the perovskite structure. In fact, $NaFeF_3$ has been shown to distort to an orthorhombic symmetry structure as Atsushi Okazaki et al. [57] when they studied the crystal structures of the anti-ferromagnetic $KMnF_3$, $KFeF_3$ $KCoF_3$, $KCNiF_3$ and $KCuF_3$ have been determined above and below their Néel temperatures (T_N) by X-ray diffraction using single crystals. They have reported that all these fluorides $KMnF_3$, $KFeF_3$ $KCoF_3$, $KNiF_3$ and $KCuF_3$ exhibit the ideal perovskite type (cubic) except for that of $KCuF_3$ Which adopts a (tetragonal) modification (a > c) of the perovskite type.

Table2.a: Lattice Pm-3m Cubic parameters for $KCoF_3$ Fluoride on the Non-Ferromagnetic (NF) and Ferromagnetic (FM) configurations using different approaches compared with theoretical and experimental work.
i: Ref [101],l: Ref [104], a: Ref [105], n: Ref [106], o: Ref [107],p: Ref [108], q: Ref [109].

$KCoF_3$							
Approach	Configuration	a_0(Å)	c_0(Å)	B (GPa)	B'	Vol(Å^3)	Phase
LDA	*Non-Ferromagnetic*	3.841	-	116.21	4.85	57.53	Cubic *Pm-3m*
LDA+U		3.879	-	117.24	4.09	58.26	
L(S)DA	*Ferromagnetic*	4.013	-	93.69	4.40	64.52	
L(S)DA+U		4.035	-	90.70	4.69	65.62	
Comparison with theoretical and experimental data							
Experimental	-	4.006[p]	-	-	-	-	Cubic *Pm-3m*
		4.069[p]	-	-	-	-	
		4.070[n]	-	-	-	-	
		4.08[q]	-	-	-	-	
Theoretical	-	4.041[a]	-	-	-	-	
		4.058[p]	-	-	-	-	
		4.069[l,o]	-	-	-	-	
		4.070[i]	-	-	-	-	
		4.071[i]	-	-	-	-	
		4.125[a]	-	-	-	-	

Table2.b: Lattice 4H-layered Hexagonal (P6/mmc) parameters for $KCoF_3$ Fluoride on the Non-Ferromagnetic (NF) and Ferromagnetic (FM) configurations using different approaches compared with theoretical and experimental work.

Approach	Configuration	a_0(Å)	c_0(Å)	B (GPa)	B'	Vol(Å^3)	Phase
LDA	*Non-Ferromagnetic*	5.517	8.754	113.39	3.937	1669.14	4H-Hexa-gonal
LDA+U		5.518	8.756	104.81	4.58	1674.36	
L(S)DA	*Ferromagnetic*	5.635	8.941	58.58	7.929	1743.49	
L(S)DA+U		5.647	8.960	97.41	6.640	1785.94	

Table2.c: Lattice Orthorhombic (Pnma) parameters for $KCoF_3$ Fluoride on the Non-Ferromagnetic (NF) and Ferromagnetic (FM) configurations using different approaches compared with theoretical and experimental work.

Approach	Configuration	a_0(Å)	c_0(Å)	B (GPa)	B'	Vol(Å^3)	Phase
LDA	Non-Ferromagnetic	5.486	7.628	5.475	117.3	4.6	Pnma Ortho-rhombic
LDA+U		5.430	7.794	5.419	117.4	4.6	
L(S)DA	Ferromagnetic	5.630	7.822	5.532	104.9	3.4	
L(S)DA+U		6.150	8.544	5.684	96.2	4.3	

To investigate the interplay between the transition phases which allows a new crystal structure to be done and B-site stereo chemical activity, three crystallographic models (Figure. 1.a), were chosen: cubic (Pm-3m), which allows neither octahedral rotations nor B-site off-centering. The crystallographic data for ABX_3 is well known and available from the literature. The crystal structure belongs to the space group (Pm-3m) (221) with the A (K atom) are in Wyckoff position 1b (½,½,½); the B (Fe, Co, and Ni atoms) in 1a (0,0,0); and the X (F atom) in 3d (½,0,0); (0,½,0);(0,0,½), all special positions.

Table3.a: Lattice Pm-3m Cubic parameters for $KNiF_3$ Fluoride on the Non-Ferromagnetic (NF) and Ferromagnetic (FM) configurations using different approaches compared with theoretical and experimental work.
j: Ref [102], k: Ref [103], l: Ref [104], n: Ref [106], q: Ref [109], r: Ref [110], s: Ref [111], t: Ref [112], u: Ref [113], f, v: Ref [114].

$KNiF_3$							
Approach	Configuration	a_0(Å)	c_0(Å)	B (GPa)	B'	Vol(Å^3)	Phase
LDA	*Non-Ferromagnetic*	3.863	-	115.73	5.04	57.65	Cubic *Pm-3m*
LDA+U		3.861	-	116.89	4.73	57.55	
L(S)DA	*Ferromagnetic*	3.954	-	91.02	3.39	61.86	
L(S)DA+U		3.974	-	97.73	4.33	62.73	
Comparaison with theoretical and experimental data							
Experimental	-	4.000[s]	-	-	-	-	Cubic *Pm-3m*
		4.02[n]	-	-	-	-	
		4.011[v]	-	-	-	-	
Theoretical	-	4.000[s]	-	-	-	-	
		4.001[t]	-	-	-	-	
		4.002[u]	-	-	-	-	
		4.009[k]	-	-	-	-	
		4.011[l]	-	-	-	-	
		4.012[e, j]	-	-	-	-	
		4.013[k]	-	-	-	-	
		4.014[v,r]	-	-	-	-	
		4.015[t]	-	-	-	-	
		4.034[k]	-	-	-	-	
		4.054[f]	-	-	-	-	
		4.070[q]	-	-	-	-	

Table3.b: Lattice 4H-Hexagonal (P6/mmc) parameters for $KNiF_3$ Fluoride on the Non-Ferromagnetic (NF) and Ferromagnetic (FM) configurations using different approaches compared with theoretical and experimental work.

Approach	Configuration	a_0(Å)	c_0(Å)	B (GPa)	B'	Vol(Å^3)	Phase
LDA	*Non-*	5.549	8.804	110.36	3.64	1698.28	4H-
LDA+U	*Ferromagnetic*	5.550	8.805	110.45	3.63	1699.15	Hexa-
L(S)DA	*Ferromagnetic*	5.596	8.880	93.97	4.492	1750.57	gonal
L(S)DA+U		5.607	8.897	93.40	4.54	1760.55	*P6/mmc*

Table3.c: Lattice Pnma-Orthorhombic parameters for $KNiF_3$ Fluoride on the Non-Ferromagnetic (NF) and Ferromagnetic (FM) configurations using different approaches compared with theoretical and experimental work.

Approach	Configuration	a_0(Å)	c_0(Å)	B (GPa)	B'	Vol(Å^3)	Phase
LDA	*Non-*	5.512	7.734	5.465	112.4	4.7	
LDA+U	*Ferromagnetic*	5.721	8.092	5.467	112.2	4.7	Ortho-
L(S)DA	*Ferromagnetic*	5.584	7.868	5.427	104.7	4.3	rhmbic
L(S)DA+U		5.787	8.079	5.771	102.1	4.5	Pnma

The perovskite structure is known to be very flexible and the A and B ions can be varied leading to the large number of known compounds with perovskite or related structures. Most perovskites are distorted and do not have the ideal cubic structure [58]. A variety of scientific works have considered the cubic structure with (Pm-3m) space group is that which Fluoro-perovskites $KFeF_3$ adopts [59-63]. M. SAFA et al [64], have also confirmed the cubic phase for the Fluorides $KFeF_3$, $KCoF_3$, and $KNiF_3$ crystals studied in their work at room temperature become antiferromagnetic (AF) above liquid nitrogen temperature. As they are good examples of simple Heisenberg magnets large crystals have been required for a variety of magnetic measurements. In other hand M. P. J. Punkkinen [65] Shows that both $KFeF_3$, $KCoF_3$ fluorides are known to exhibit (AF) insulators. He used the density functional theory in the local (spin) density approximation (LDA/LSDA) to predict the metallic behavior for these fluorides. A. S. Verma in different works as well many other researchers have given wide attention to this type of Fluorides [66-74] because they show specific physical properties due to their crystal structures and unique ferroelectric dielectric, (anti)magnetic and optoelectronic properties. Revised structural phase transition are made in $KMnF_3$ Fluoro-perovskite crystals as well as Joanna Kapusta et al. [75] works, and many other scientist researchers have also mentioned that exist structural phase transition in the $KMnF_3$ Fluorides (Mn are transition metals) [76-82] which has been considered cubic for a very long time, critical behavior magnetic transitions are given specially for two $KCoF_3$ and $KNiF_3$ Fluorides by A. Oleaga et al. [83], also Atsushi Okazaki et al. [57] studied the crystal structures of the anti-ferromagnetic $KMnF_3$, $KFeF_3$ $KCoF_3$, $KCNiF_3$ and $KCuF_3$ have been determined above

and below their Néel temperatures (T_N) by X-ray diffraction using single crystals. They reported that the structures of these compounds are the ideal perovskite type (cubic) except for that of $KCuF_3$ Which crystallizes as a tetragonal modification (a > c) of the perovskite type. At 78°K (below T_N) the lattice symmetries of $KMnF_3$, $KFeF_3$ and $KCoF_3$ are monoclinic, rhombohedral (α<90°) and tetragonal (a > c), respectively, while $KNiF_3$ and $KCuF_3$ retain their own symmetries at room temperature was extended up to 670°K for $KCuF_3$. S. L. Wang et al [84] reported that KMF_3 with (M= Mn, Co, and Ni) after be synthesized through a simple solution route, these compounds crystallized in a cubic perovskite phase (Pm-3m). The crystal structure of KMF_3 was refined by the Rietveld method on the basis of the X-ray powder diffraction data. S. L. Wang et al reported that the typical compound KMF_3 (M: Transition Metal) shows that the magnetic properties and spin configuration can be changed by the crystal structure itself and external conditions (Dovesi et al. 1997 [85]). The cubic room temperature perovskite structure of $KMnF_3$ transforms to an orthorhombic phase at 184 K (Beckman and Knox, 1961 [86], Kizhaev and Markova 2011 [87]) and transition into tetragonal phase (P4/mbm) at 91.5 K (Du et al (2005) [88], Salje et al (2009) [89]). The change of structure causes a transition to uniaxial (AF) below 88.3 K (Heeger et al (1961) [90]). For perovskite-type Cobalt Fluoride $KCoF_3$ the crystal structure is slightly distorted and its spin state is changed with temperature shift. From all these studies we can concluded that all these fluorides undergo phase transition due to the change in temperature or to the pressure exerted, and this appears clearly in the magnetic behavior and the spin configuration investigation studies. Using the classical approximations (L(S)DA) invested largely in the ab-initio calculation, we show these phase transition by the investigation of the Four-Layered 4H-Hexagonal (P6/mmc), and the (Pnma) Orthorhombic phase vs Cubic (Pm-3m) crystal phase for KFeF3, KCoF3 and KNiF3 Fluorides using (L(S)DA) vs (L(S)DA+U) approaches where we included the U-Hubbard correction to correctly description for the ground states properties and magnetic effect on these fluorides to show also the cation effect. (Figure. 1.b), displays the Four-Layered 4H-Hexagonal (P6/mmc), which allows for simultaneous octahedral rotations and B-site off-centering along the c-axis. The positions are given as: A_1 = K (0, 0, 0), A_2 = K (1/3, 1/3, 1/4), B = (Fe, Co, and Ni) (1/3, 2/3, 0.6142), F_1 (0, 0, 1/2), and F_2 (-0.6129, -1.2258, 1/4). Finally, we illustrate the Orthorhombic (Pnma) phase in (Figure. 1.c), where the atomic position is taken as: A_1 = K (0.0304, 0.25, 0.99), B = (Fe, Co, and Ni) in (0, 0, 0.5), F_1 (0.449, 0.25, 0.0587), and F_2 (0.2825, 0.0366, 0.7088). We aim in this part to calculate the total energy as a function of unit-cell volume around the equilibrium cell volume V_0. The calculated total energies versus

volume as shown in (Figure. 2.a), (Figure. 2.b), and (Figure. 2.c), are fitted with the Murnaghan equation of state [91]. We present the computed total energy versus unit-cell volume for the $KFeF_3$, $KCoF_3$ and $KNiF_3$ Fluoro-perovskites with L(S)DA and L(S)DA+U respectively for two configurations Non-Ferromagnetic (NF) and Ferromagnetic (FM) for each fluoride separately, with (Cubic, 4H, and Orthorhombic) structures are regrouped.

Table 4.a: Magnetic moment values for $KFeF_3$ Fluoride on the Cubic (Pm-3m) phase.

Cubic Phase (Pm-3m)						
Fluoride	Approches	μK	μM	μF	$\mu_{interstitiel}$	μ_{Cell}
	L(S)DA	-0.0014	3.333	0.088	0.392	3.812
	L(S)DA+U	-0.0024	3.522	0.068	0.272	3.860

Table 4.b: Magnetic moment values for $KFeF_3$ Fluoride on the 4H-Hexagonal (P6/mmc) phase.

	4H-Hexagonal Phase (P6/mmc)							
Fluoride	Approches	μA_1	μA_2	μB	μF_1	μF_2	$\mu i_{nterstitiel}$	μ_{Cell}
	L(S)DA	0.0011	-0.0004	3.399	0.106	0.108	1.111	4.733
	L(S)DA+U	0.0007	-0.0002	3.408	0.096	0.100	1.183	4.787

Table 4.c: Magnetic moment values for $KFeF_3$ Fluoride on the Orthorhombic (Pnma) phase.

Orthrhombic Phase (Pnma)							
Fluoride	Approches	μA	μB	μF_1	μF_2	$\mu_{interstitiel}$	μ_{Cell}
	L(S)DA	-0.0020	3.411	0.098	0.092	1.139	4.738
	L(S)DA+U	-0.0011	3.543	0.057	0.053	1.112	4.764

Table 5.a: Magnetic moment values for $KCoF_3$ Fluoride on the Cubic (Pm-3m) phase.

Cubic Phase (Pm-3m)						
Fluoride	Approches	μ_K	μ_M	μ_F	$\mu_{interstitiel}$	μ_{Cell}
	L(S)DA	-0.0016	2.345	0.093	0.139	2.575
	L(S)DA+U	-0.0014	2.663	0.079	0.102	2.843

Table 5.b: Magnetic moment values for $KCoF_3$ Fluoride on the 4H-Hexagonal (P6/mmc) phase.

	4H-Hexagonal Phase (P6/mmc)							
Fluoride	Approches	μA_1	μA_2	μB	μF_1	μF_2	$\mu_{interstitiel}$	μ_{Cell}
$KCoF_3$								
	L(S)DA	0.0020	0.0001	1.581	0.028	0.076	0.329	2.016
	L(S)DA+U	0.0011	-0.0002	2.552	0.099	0.117	0.492	3.260

Table5.c: Magnetic moment values for $KCoF_3$ Fluoride on the Orthorhombic (Pnma) phase.

Orthorhombic Phase (Pnma)							
Fluoride	Approches	μA	μB	μF_1	μF_2	$\mu_{interstitiel}$	μ_{Cell}
$KCoF_3$	L(S)DA	-0.0006	2.568	0.102	0.096	0.545	3.310
	L(S)DA+U	-0.0008	2.698	0.049	0.051	0.560	3.357

Table 6.a: Magnetic moment values for $KNiF_3$ Fluoride on the Cubic (Pm-3m) phase.

vCubic Phase (Pm-3m)						
Fluoride	Approches	μ_K	μ_M	μ_F	$\mu_{interstitiel}$	μ_{Cell}
	L(S)DA	-0.0012	1.411	0.076	0.050	1.536
	L(S)DA+U	-0.0005	1.773	0.054	0.064	1.891

Table 6.b: Magnetic moment values for $KNiF_3$ Fluoride on the 4H-Hexagonal (P6/mmc) phase.

	4H-Hexagonal (P6/mmc)							
Fluoride	Approches	μA_1	μA_2	μB	μF_1	μF_2	$\mu_{interstitiel}$	μ_{Cell}
	L(S)DA	0.0022	-0.0006	1.634	0.085	0.131	0.002	1.853
	L(S)DA+U	0.0011	-0.0005	1.634	0.080	0.130	0.198	2.043

Table 6.c: Magnetic moment values for $KNiF_3$ Fluoride on the Orthorhombic (Pnma) phase.

Orthorhombic (Pnma)							
Fluoride	Approches	μA	μB	μF_1	μF_2	$\mu_{interstitiel}$	μ_{Cell}
$KNiF_3$	L(S)DA	-0.0001	1.642	0.094	0.101	0.188	2.025
	L(S)DA+U	-0.0006	1.802	0.046	0.047	0.181	2.076

2. B. Computational Methods

Our calculations have been performed with the Wien2K Ab-initio Simulation Package [92] implementing the projector Full-Potential Linear Augmented Plane waves method [93-94] embedded in the functional (DFT+U) basis [44, 45]. (DFT+U) is employed for all open shell orbitals, such as *d* and *f* orbitals for transition metal elements with localized orbitals existing in extended states, as in the case of many strongly correlated materials and perovskites, where localized *3d* or *4f* orbitals are embedded in elongated *s-p* states [95]. In the FP-LAPW method, the unit cell is divided into two parts: (I) non-overlapping atomic spheres (centered at the atomic sites) and (II) an interstitial region. In this method no shape approximation on either the potential or electronic charge density is made. It allows the

inclusion of local orbitals in the basis, we are improving upon linearization and making possible a consistent treatment of semi-core and valence states. This is an implementation of a hybrid full potential linear augmented plane wave within local orbitals (L/APW+*lo*) method given in the Wien 2K package. The basis set inside each MT sphere is split into core and valence subsets. The core states are treated within the spherical part of the potential only and are assumed to have a spherically symmetric charge density totally confined inside the MT spheres. Two different approaches are employed in the present work to describe the exchange and correlation potential interaction, such as (Perdew-Wang) local spin density approximation LSDA [58-59] and corrected LSDA+U [96-97]. Therefore, applying U-Hubbard correction to solve the bandgap problem is necessary for predicting the properties of transition metal oxides. The (DFT+U) description is accurate method to interpret the ground states properties for materials. The applications of the U value is not known and practically is often tuned semi empirically to make a good agreement with experimental or higher level computational results. However, the semi empirical way of evaluating the U parameter fails to capture its dependence on the volume, structure, or the magnetic phase of the crystal, and also does not permit the capturing of changes in the on-site electronic interaction under changing physical conditions, such as chemical reactions[95]. The value of U implemented by Cococcioni et al. [95, 98] is U_{eff} = U−J, where J is indirectly assumed to be zero in order to obtain a simplified expression. Nonetheless, J can add some additional flexibility to the (DFT+U) calculations, but it may yield surprising results including reversing the trends previously obtained in the implemented (DFT+U) calculations [95]. To ensure convergence we have taken 2000K points in the Brouillin Zone. The self-consistent calculations are considered to be converged only when the calculated total energy of the crystal converged to less than 1 mRy. In this work, we have chosen for the (L(S)DA) vs (L(S)DA+U) calculation, the on-site effective U parameter is (U_{eff} U-J= 0.47 eV). We have chosen as atomic sphere radii (RMT) 2.4, 1.9, and 1.6 a.u respectively for A, B (Fe, Co, and Ni) and F atoms. The Brillouin Zone integration is carried out with a modified tetrahedron method [99]. In order to describe correctly the wave functions in the interstitial region like spherical harmonics have been expanded up to the value of l_{max}=7. (DFT+U) are good to predict the correlation in the centered metal in organometallics. The spin change between FM and AFM states or in SCO can all be well predicted by the Hubbard correction, while the pure (DFT) fails due to the correlation in the *d* or *f* orbitals of the centered metal [95], these characteristics, and the advantages that it can allow us justifies the integration of this method in the present paper. We qualify this method according to our results presented below as an accurate method.

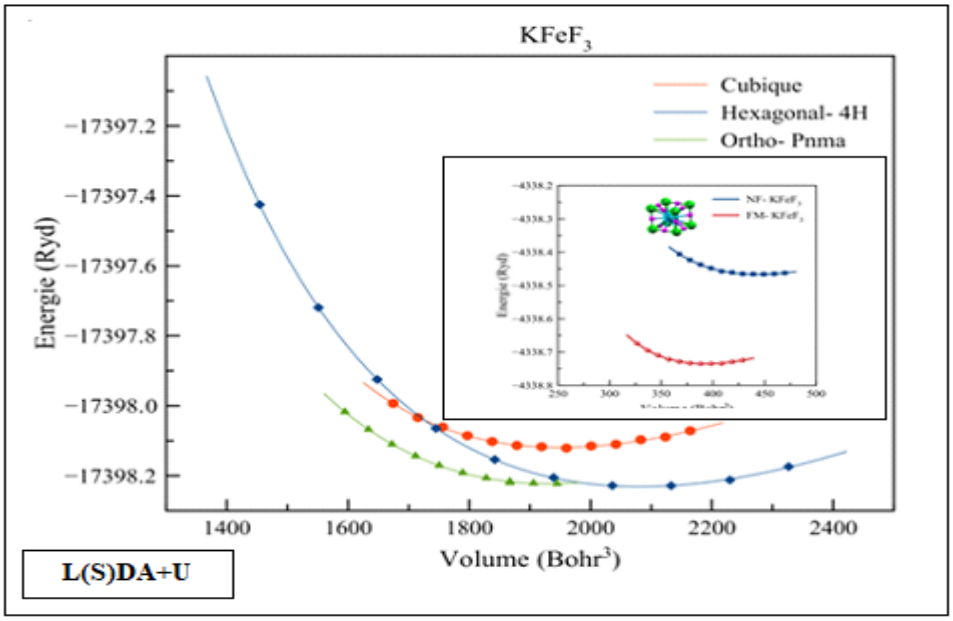

Figure 2a. Computed total energy versus unit-cell volume for the Cubic $KFeF_3$ Fluoro-perovskites with L(S)DA+U approach.

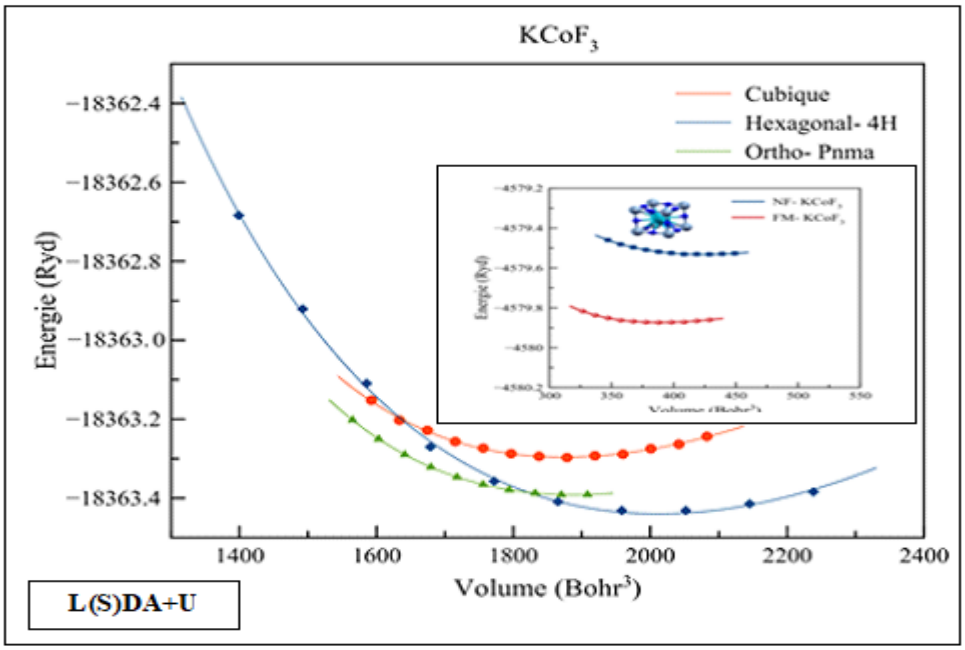

Figure 2b. Computed total energy versus unit-cell volume for the Cubic $KCoF_3$ Fluoro-perovskites with L(S)DA+U approach.

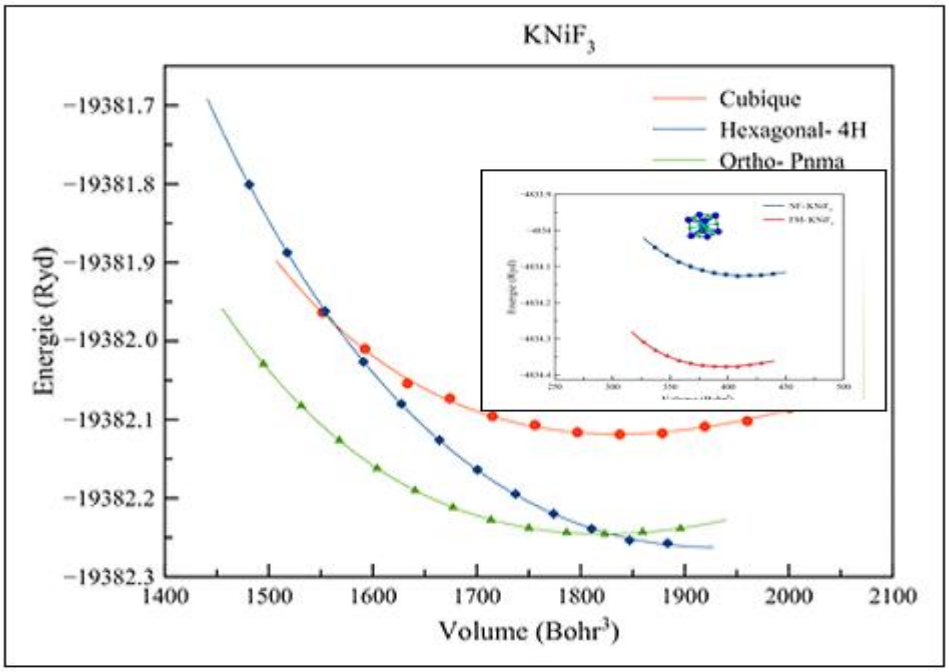

Figure 2c. Computed total energy versus unit-cell volume for the Cubic $KNiF_3$ Fluoro-perovskites with L(S)DA+U approach.

3. Results and Discussions

3. A. Structural properties and Magnetic moment

To obtain an analytical interpolation of our computed points from which we determine the ground state properties such as the equilibrium lattice constant a_0 (Â), or c_0(Â), the bulk modulus B(GPa) and its pressure derivative B_0. We present in (Table. 1.a), (Table. 2.a), and (Table. 3.a) the computed (LDA) and (LDA+U) for (NF) configuration as well (LSDA) and (LSDA+U) for (FM) configuration for $KFeF_3$, $KCoF_3$ and $KNiF_3$ respectively. The equilibrium lattices are given together with other theoretical and experimental values. In this work, the equilibrium lattice constants for the cubic KBF_3 Fluoride are underestimated by (L(S)DA) and overestimated by (L(S)DA+U), which are perfectly near the theoretical and experimental works given by others researchers. (Table. 1.b), (Table. 2.b), and (Table. 3.b) show the lattice equilibrium for the 4H-phase. We report for $KFeF_3$ a= 4.033 Â, $KCoF_3$ a= 4.035Â and for $KNiF_3$ a=3.974 Â for the Ferromagnetic (FM) configuration. For the 4H-Hexagonal Fluorides, the sub-cell lattice constants are: $KFeF_3$ (a=5.727Â, c= 9.086Â); $KCoF_3$ (a=5.647Â, c=8.960Â), and for $KNiF_3$ (a=5.607Â, c=8.897Â), while in the Pnma orthorhombic phase we report these lattices $KFeF_3$ (a=5.828Â, c=8.594Â); $KCoF_3$

(a=6.150Â, c=8.544Â), and for $KNiF_3$ (a=5.787Â, c=8.079Â). The equilibrium values for the Pnma-Orthorhombic structure are given in (Table. 1.c), (Table. 2.c), and (Table. 3.c). From (Figure.2.a), (Figure.2.b), and (Figure.2.c), we deduce that the computed total energy versus unit-cell volume for the KBF_3 (B=Fe, Ni, and Co) Fluoro-perovskites with (LDA+U) respectively for two configurations Non-Ferromagnetic (NF) and Ferromagnetic (FM) shows the Ferromagnetic (FM) behavior. The three $KFeF_3$, $KCoF_3$ and $KNiF_3$ Fluorides investigated here are (FM). While the other curve which brings together all the structures (Cubic, 4H, and Orthorhombic) for $KFeF_3$, $KCoF_3$ and $KNiF_3$ Fluorides shows that there is an intersection interval between the two crystal structures (4H- Hexagonal and Orthorhombic), after they adopt the 4H-Hexagonal structure. This remark is explained by a transition phase that these fluorides undergo during a change of temperature or it is due to a pressure exerted on them. We report in (Table.4.a), (Table.5.a), and (Table.6.a) the magnetic moment for the (Cubic, 4H, and Orthorhombic) $KFeF_3$ Fluorides respectively. The $KCoF_3$ magnetic moment are reported respectively in (Table.4.b), (Table.5.b), and (Table.6.b) The $KNiF_3$ magnetic moment are reported in (Table.4.c), (Table.5.c), and (Table.6.c) respectively. From these figure, we see clearly that the Potassium K contribution is negligible. We found an important magnetic moment contribution given by the second element (B=Fe, Co, Ni) respectively. we classify it according to this order (Fe, Co, and Ni). This this classification leads us to say that our fluorides are classified as $KFeF_3$> $KCoF_3$> $KNiF_3$. This contribution appears clearly in the band structure and densities of states plots given after.

4. Electronic properties

4. A. Densities of states and Band structure

The (FP-LAPW) is a good theoretical tool for the calculation of the electronic properties of a compound. They give useful information about the internal perovskite structure as well as Fluoro-perovskites. We turn our attention in this part to study the electronic properties of three $KFeF_3$, $KCoF_3$ and $KNiF_3$ Fluorides via calculating the energy band structure the total and partial densities of states and the charge distribution. (Figure.3.a), (Fig.ure3.b), (Figure.3.c) show band structures within (L(S)DA) and (L(S)DA+U) respectively for Cubic (Pm-3m) phase, where (Figure.4.a), (Fig.ure4.b), (Figure.4.c) show the total and partial densities of states for this phase. The band Structure and total and partial densities of states for the Four-layered Hexagonal (4H) phase is given in (Figure.5.a), (Fig.ure5.b), (Figure.5.c) respectively. The Fermi level is fixed at the origin. It is well known

that the (L(S)DA) approach underestimate the fundamental gap of semiconductors and insulators.

The introduction of the U-Hubbard term is essential, we found that (L(S)DA+U) approach gives us more information.

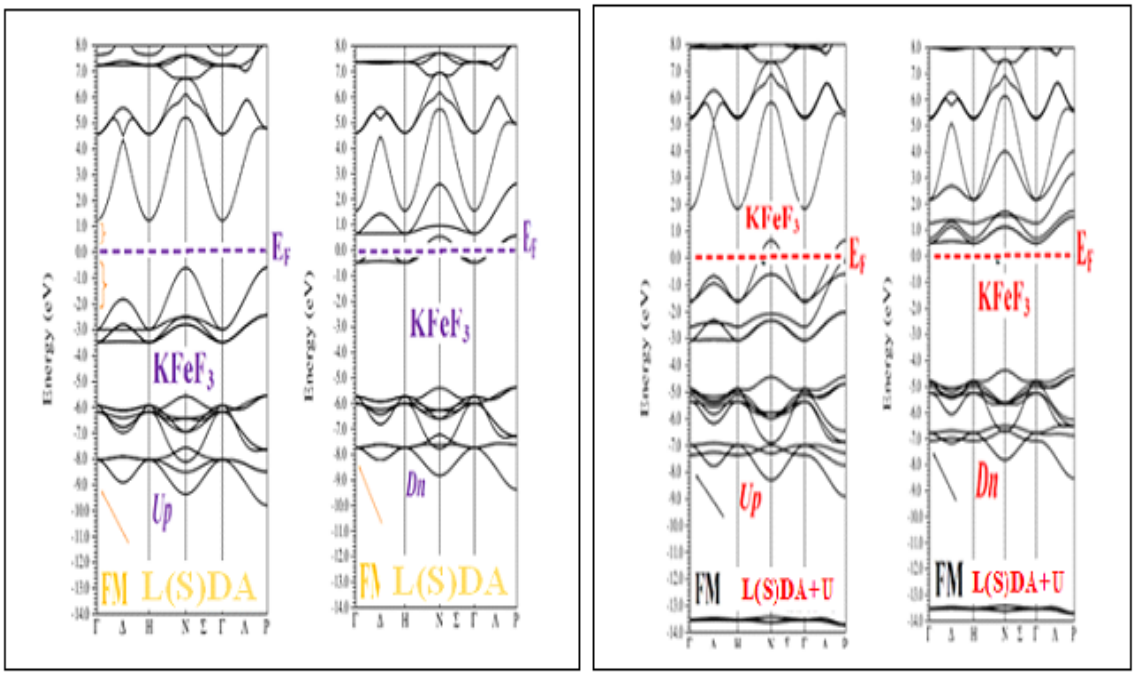

Figure 3a. Band Structures for the Cubic $KFeF_3$ Fluorides with (L(S)DA) and (L(S)DA+U) respectively.

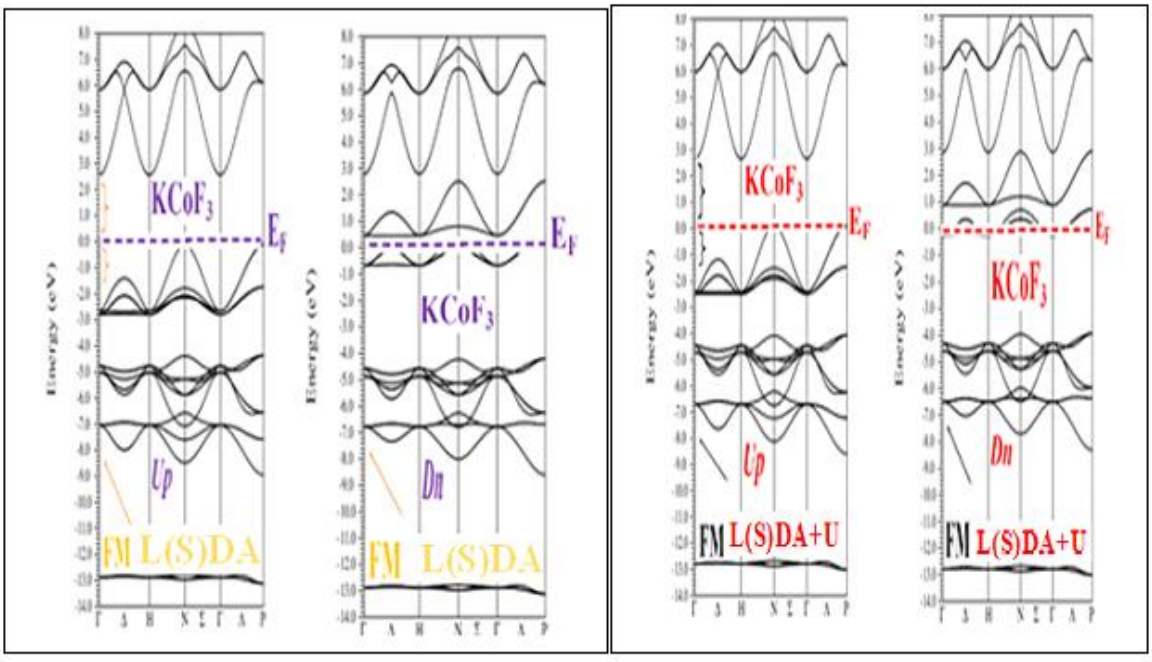

Figure 3b. Band Structures for the Cubic $KCoF_3$ Fluorides with (L(S)DA) and (L(S)DA+U) respectively.

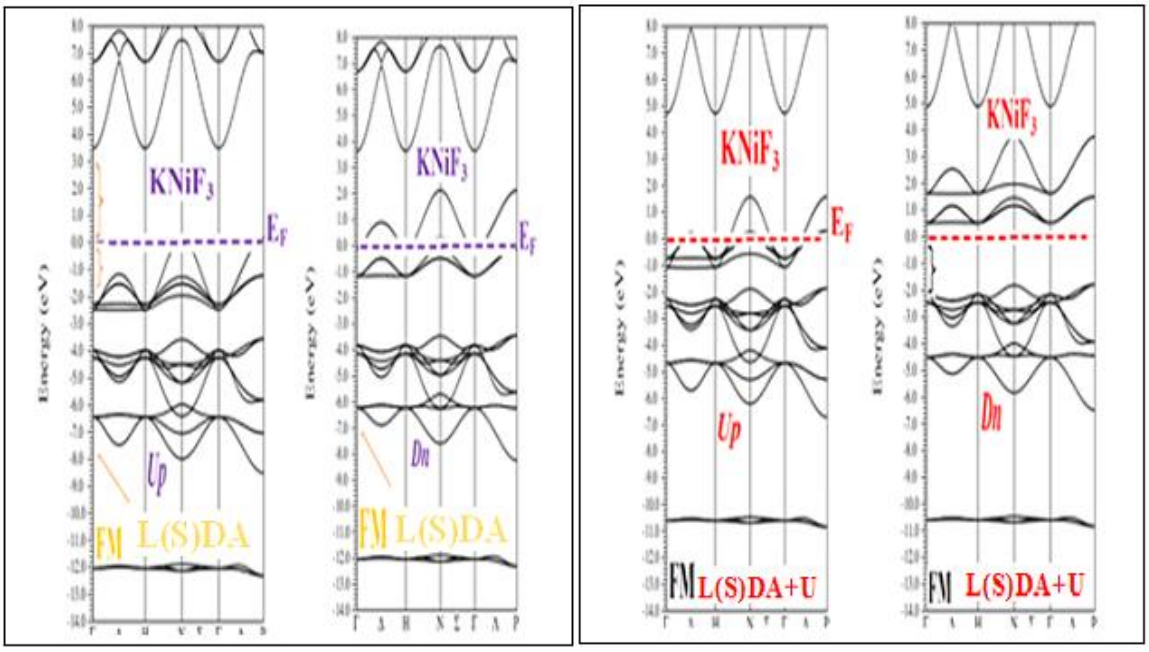

Figure 3c. Band Structures for the Cubic $KNiF_3$ Fluorides with (L(S)DA) and (L(S)DA+U) respectively.

The (L(S)DA+U) method is able to predict the electromagnetic properties. Further, the values of the magnetic moments are in better agreement with other theoretical and experimental values in the (L(S)DA+U) calculations than in the (L(S)DA) calculations. The energy band gap of KBF_3 Fluorides with (B= Fe, Co, and Ni) along N-Γ is indirect gap. The energy band gap shows differences between U_P-states and *Dn*-states. The Cubic value of (L(S)DA+U) for $KFeF_3$, $KCoF_3$ and $KNiF_3$ Fluorides respectively are overestimated than the (L(S)DA) values given as $KFeF_3$, $KCoF_3$ and $KNiF_3$ Fluorides. The same remark is obtained in the Four-layered 4H-Hexagonal and orthorhombic phases. It is worth noting that the (L(S)DA) given here usually underestimates the band gap. The conduction band is dominated by *d*-Fe states or *d*-Ni as *d*-Co, and the band gap. The calculated electronic band structure reveals that KBF_3 studied here is an insulator similar to other Fluoro-perovskite studied by different researchers [84, 100, 101] as well is given in Total (TDOS) and partial densities of states (PDOS) in the cubic phase shown in (Fig.4). The insulator behavior exists in all these fluorides. The top valence bands of Fluorides are mainly formed by the *p*-F states, the *2p*-F states are fully occupied. The bottom conduction bands are created by K and F states, and the *3d*-M states are partially occupied. We remark that in all figures given here, the studied $KFeF_3$, $KCoF_3$ and $KNiF_3$ Fluorides bands found just above the Fermi level are also mainly from the *d*-states of B atom with (B= Fe, Ni, and Co). whereas the other states K and F atoms do not contribute much to the Fermi level.

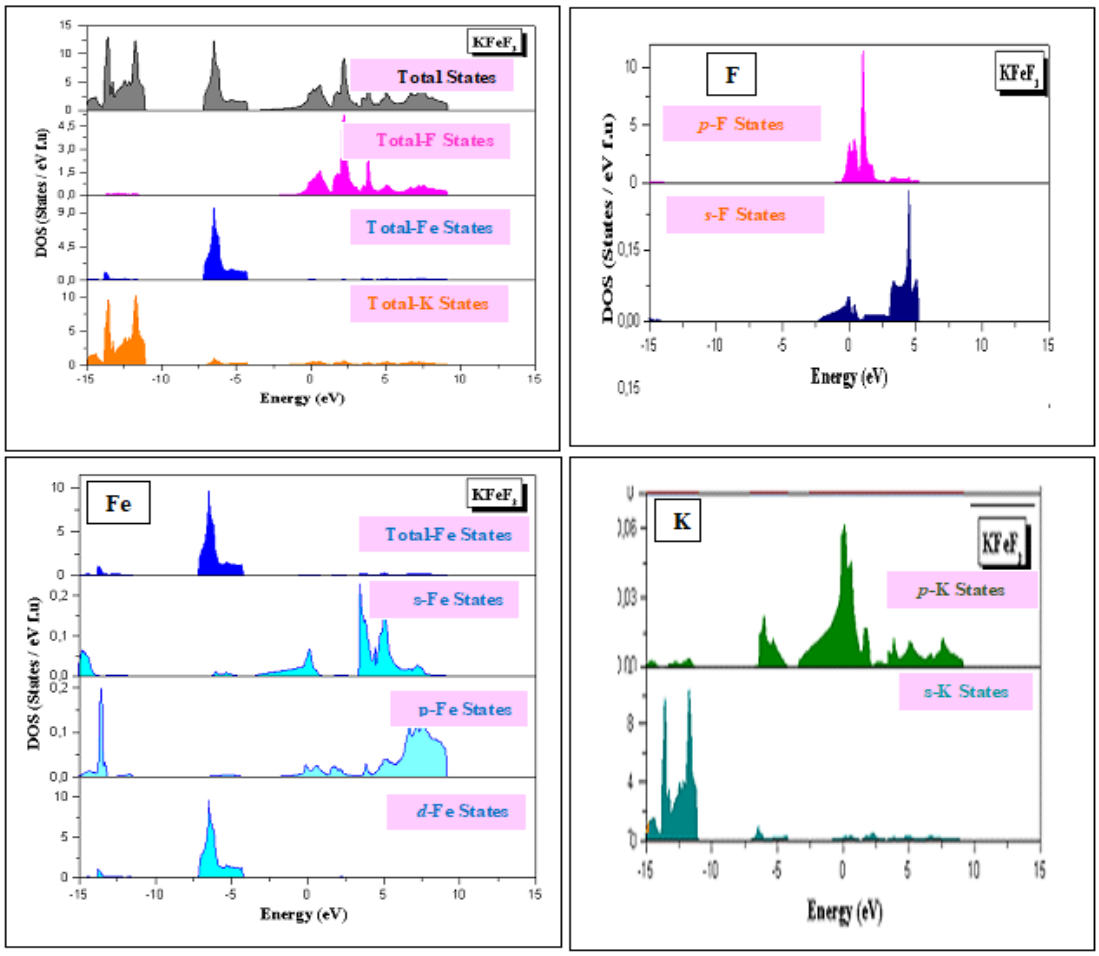

Figure 4a. Total and partial densities of states for the Cubic phase for $KFeF_3$ Fluoride with (L(S)DA+U) approaches.

The position of the last valence band sometimes exceeds the Fermi level E_F using (L(S)DA+U) approach. We note also a difference between the *Up* states and the *Dn* states, it is clear that the *Dn* states are much more descending compared to the *Up* states, they are located below the Fermi level, nearly in all the phases studied indicating the insulator character with small values in these states. We remark also that Fe contribution in $KFeF_3$ is dominated. The most remarkable thing given in the study of fluorides perovskites ABF_3 in comparison with perovskites oxides ABO_3, that fluorides show an almost similar contribution of all the elements A, B and F, especially the element B is dominant and also we found the F contribution, thing which is not found in the oxides, where the contribution of oxygen is negligible compared to the other elements, sometimes A element contributes but partially.

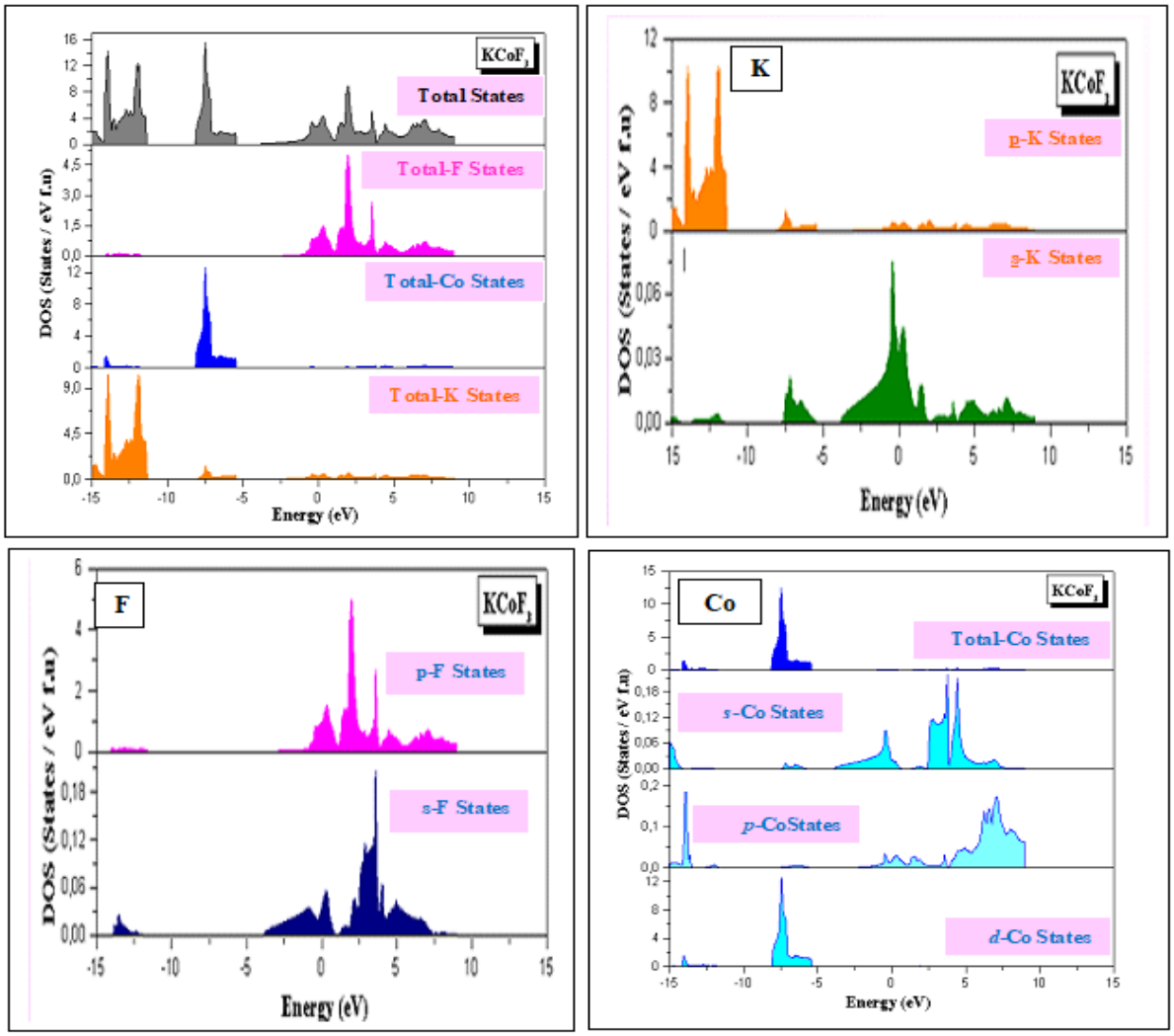

Figure 4b. Total and partial densities of states for the Cubic phase for $KCoF_3$ Fluoride with (L(S)DA+U) approaches.

The same remark is reveled in the three Fluorides studied here. we remake an equal contribution of potassium K in the three fluorides investigated here, a similar contribution of F element in $KFeF_3$ and $KCoF_3$ Fluorides, but it becomes more important in $KNiF_3$ Fluoride. From current results, we deduced that the contribution of the 2nd atom decreases as following: Co, Ni and Fe, which is completely opposite with their magnetic moment contribution which decreases as well Fe, Co, and Ni element in three phases investigated Cubic, 4H and Orthorhombic respectively. The previous study of Four-Layered Hexagonal phase in these fluorides clearly showed several different features of the band structures that point to significant covalent contributions to the bonding explained later in Charge densities part. These three types of crystal structures invested in this work, allowed us to discover the variety of physical properties that they possess these Fluorides.

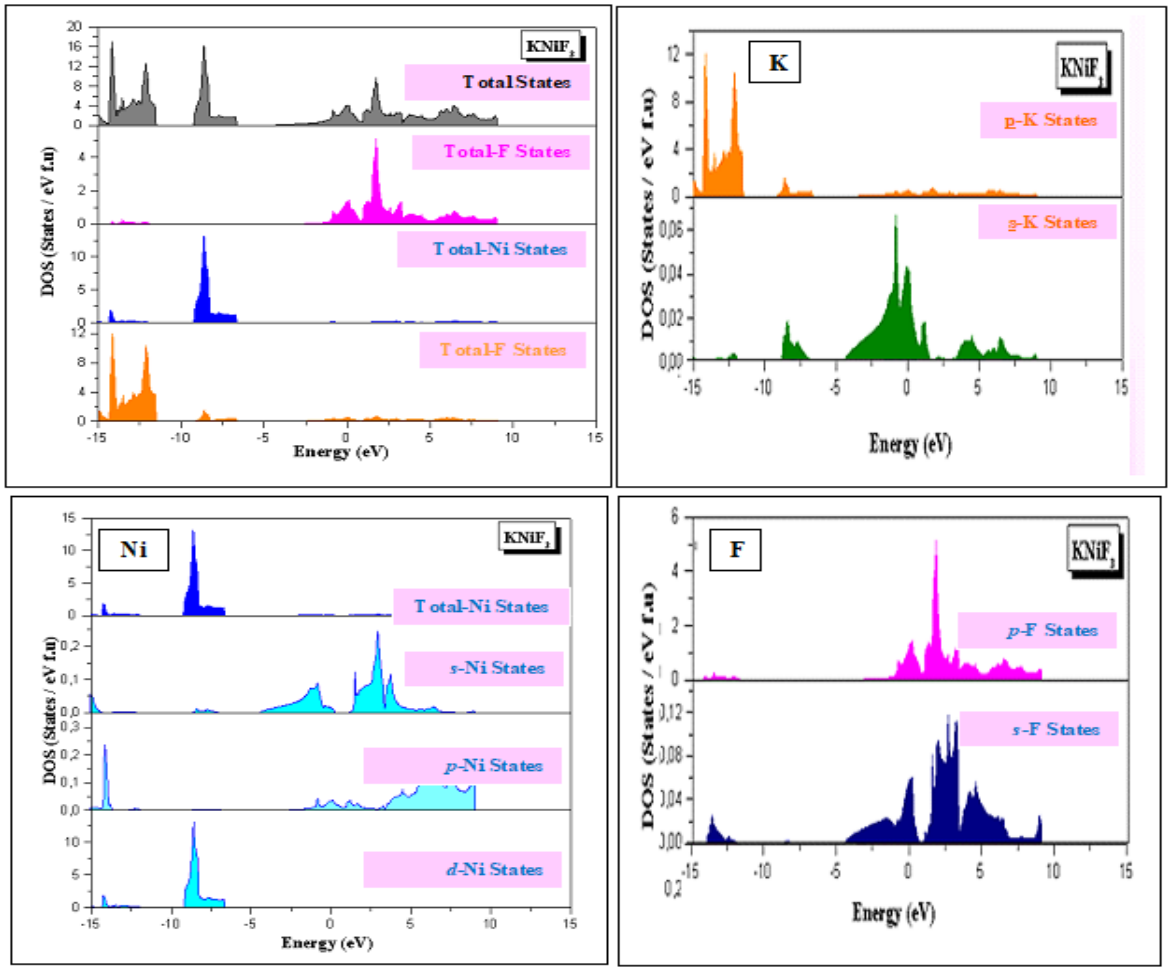

Figure 4c. Total and partial densities of states for the Cubic phase for $KNiF_3$ Fluoride with (L(S)DA+U) approaches.

The 4H-Hexagonal phase revealed that the conduction bands are raised above the Fermi level. Also Spin-Dn states are very smaller in relative to those given by Spin-Up states. In general, the band structures figures show the insulating gap which is found by many researchers in different works [102]. Partial density of state (PDOS) and total density of state (TDOS) for $KFeF_3$, $KCoF_3$ and $KNiF_3$ Fluorides in cubic phase is depicted in these figures indicates also hybridization among orbital electrons as well as bonding characteristics within the compound. Also from these figures, we see clearly that (L(S)DA+U) describe all states more than (L(S)DA) approach. The Fermi level E_F is indicated by horizontal dashed line. It is clear that several valence and conduction bands cross the E_F with large dispersion in the Dn-States the thing that was found also in the band structures, keeping the insulating character always present with a difference between the gap values from one fluoride to another which is nearly analogous to the previously reported articles.

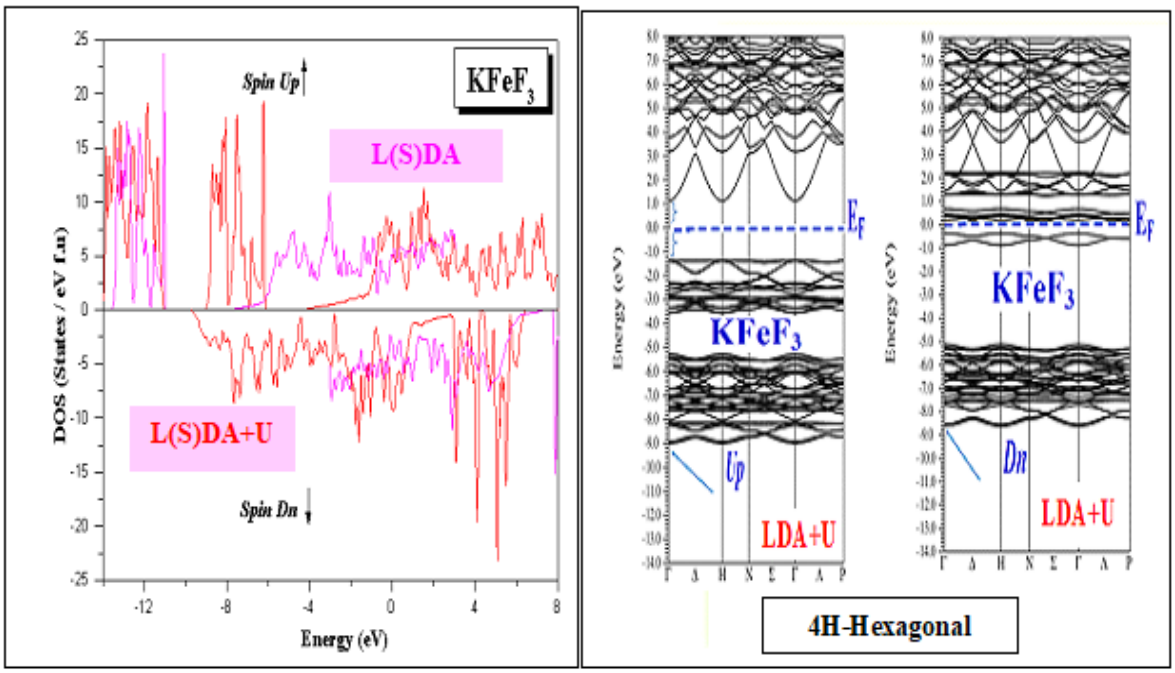

Figure 5a. Band Structure and Total and partial densities of states for the 4H-Hexagonal phase for $KFeF_3$ Fluoride with (L(S)DA) and (L(S)DA+U) approaches.

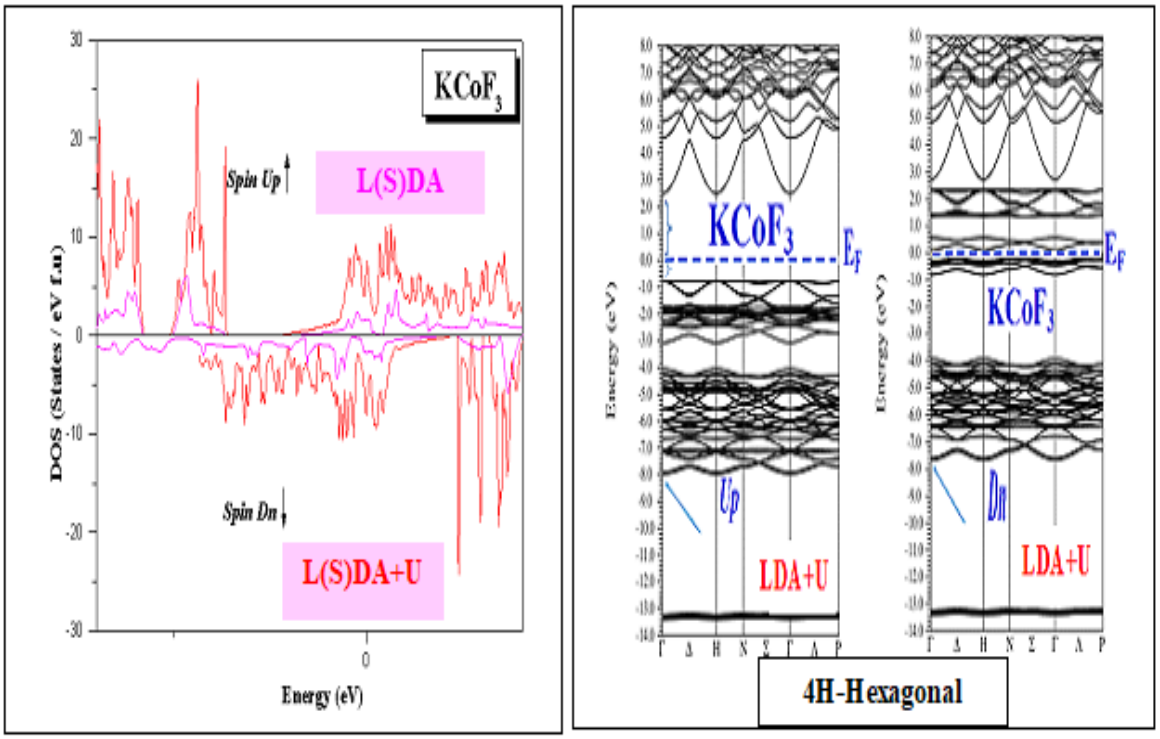

Figure 5b. Band Structure and Total and partial densities of states for the 4H-Hexagonal phase for $KCoF_3$ Fluoride with (L(S)DA) and (L(S)DA+U) approaches.

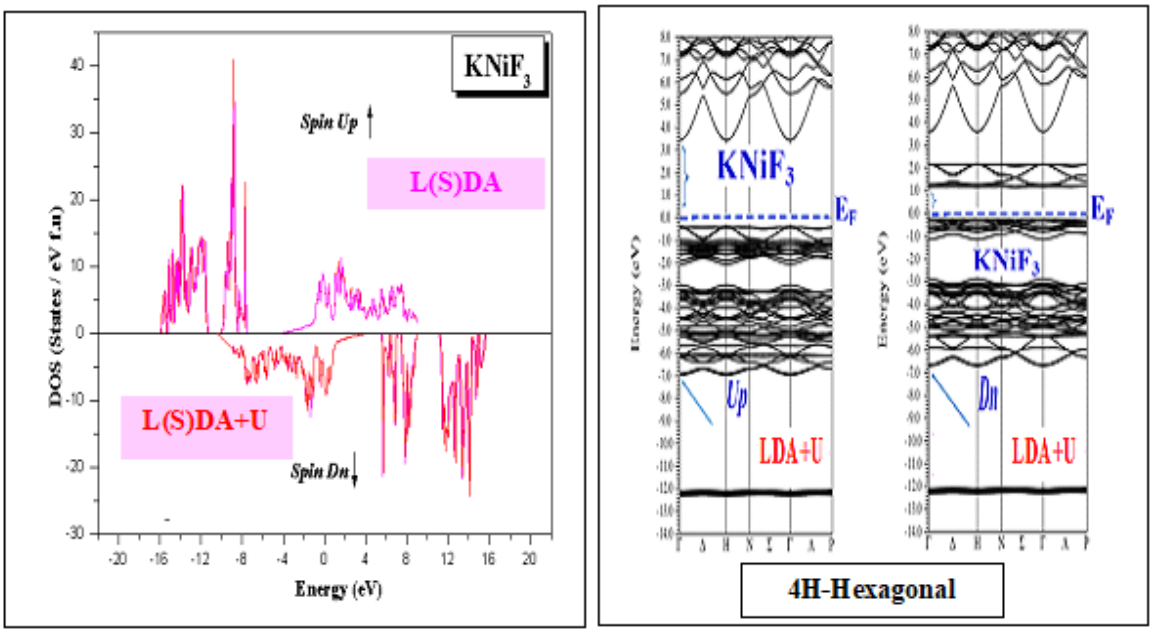

Figure 5c. Band Structure and Total and partial densities of states for the 4H-Hexagonal phase for $KNiF_3$ Fluoride with (L(S)DA) and (L(S)DA+U) approaches.

4. B. Charge densities

Charge density maps serve as a complementary tool for achieving a proper understanding of the electronic structure of the system being studied. L(S)DA+U calculations were also performed on the transfer charge in $KFeF_3$ fluoride for the cubic (Pm-3m), 4H-Hexagonal (P6/mmc) and Orthorhombic (Pnma) phases respectively. Charge density of cubic perovskites was often studied and discussed. The ionic character of any perovskite or Fluorides can be related to the charge transfer between the cation and anion elements. The covalent character is related to the sharing of the charge among the cation and anion. The covalent behavior is due to hybridization of *d*- A states and *p*-B states in the valence band near the Fermi energy level. In our case, it's due to hybridization of *d*-B states and *p*-A states because (A atom is K) we know that K element contains only *p*-states, K: [Ar] $4s^1$, it does not have the *d*-states. The *d*-states are more localized. The corresponding contour maps of the Cubic (Pm-3m) charge density distributions are shown in (Figure. 5.a) along (100) plane in 3D representation. The bond between F and F is strong ionic. We noted that Fe-Fe in $KFeF_3$ are very strong covalent Fluoride.The formation of Hexagonal perovskites given in (Figure. 5.b) is believed to be largely governed by the size misfits in the compound. The orthorhombic phase given in (Figure. c.a) contains corner-sharing octahedra only. ABF_3 Fluoro-perovskite containing intermediately sized A ion takes while the 4H-hexagonal structure which may be seen as intermediate containing both corner- and face-sharing octahedra. (Rune Sodena et al

2007) [103, 104] confirm this through their study on $SrMnO_3$ and $CaMnO_3$ perovskite oxide by showing that the hexagonal structures give more room to large alkaline-earth cations but, on the other hand, lead to short Mn-Mn distances connecting the centers of the face-sharing octahedral. They show that the face-sharing octahedra increase the electrostatic repulsion between the Mn atoms in the Mn_2O_9 entities, and therefore increase the magnitude of the Mn-Mn contribution to the Coulomb energy of the compound. The same is applied to the element B which is Fe (Ni or Co) in our fluoro-perovskites. (Rune Sodena et al 2007) [103] reported that the corresponding transition from structures containing corner-sharing octahedra to hexagonal structures with face-sharing octahedra was modeled using a set of transferable potentials within the framework of the conventional ionic model. Since these calculations allow for no change in bonding from structure to structure and no ionic contributions, the driving force for the adoption of a structure by a given fluoride is clearly size. While in both series ABF_3 and $AMnO_3$, the transition from orthorhombic to cubic to hexagonal is consistent with the increase in the tolerance factor "t". (Fig. 5) shows also along (100) plane in 3D representation the 4H-Hexagonal and Pnma-Orthorhombic transfer charge. The contribution of three elements which constitutes the ABF_3 fluoride is similar in the three crystal phases (Cubic, 4H, and Orthorhombic) studied in the current work. We find there too hybridization between the (*3d*-Fe and *2p*-F) states in the $KFeF_3$ Fluoride. We report also small differences given between the Spin-*Up* and Spin-*Dn* contribution.

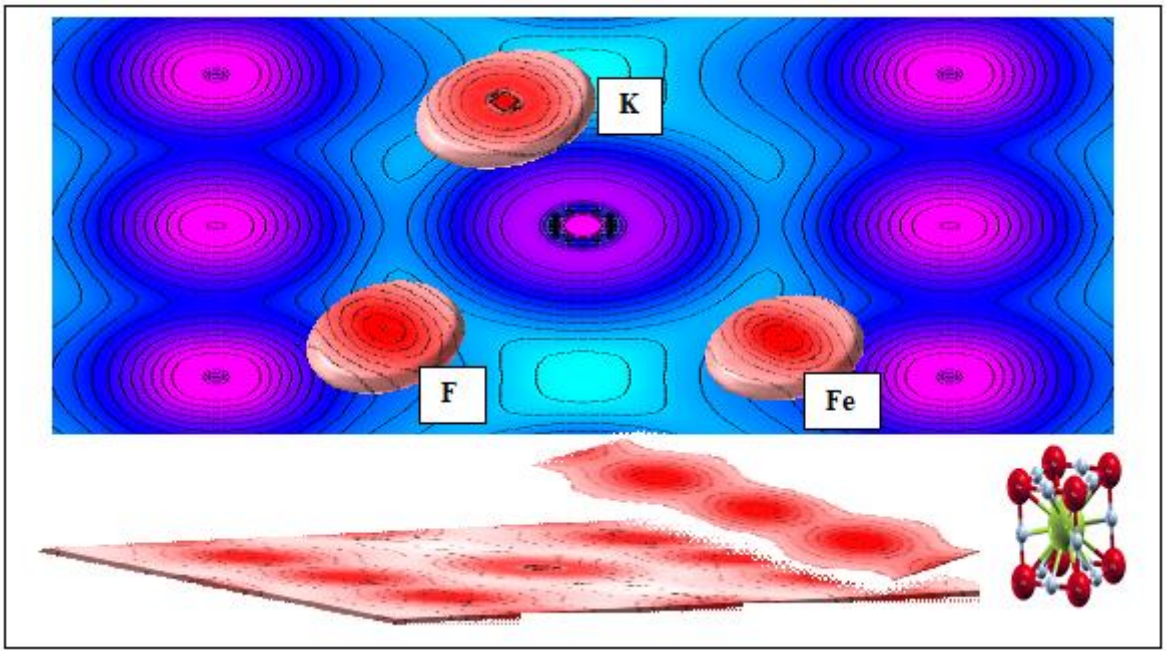

Figure 6a. Charge Densities for the Cubic (Pm-3m) phase $KFeF_3$ Fluoride with (L(S)DA+U) approach.

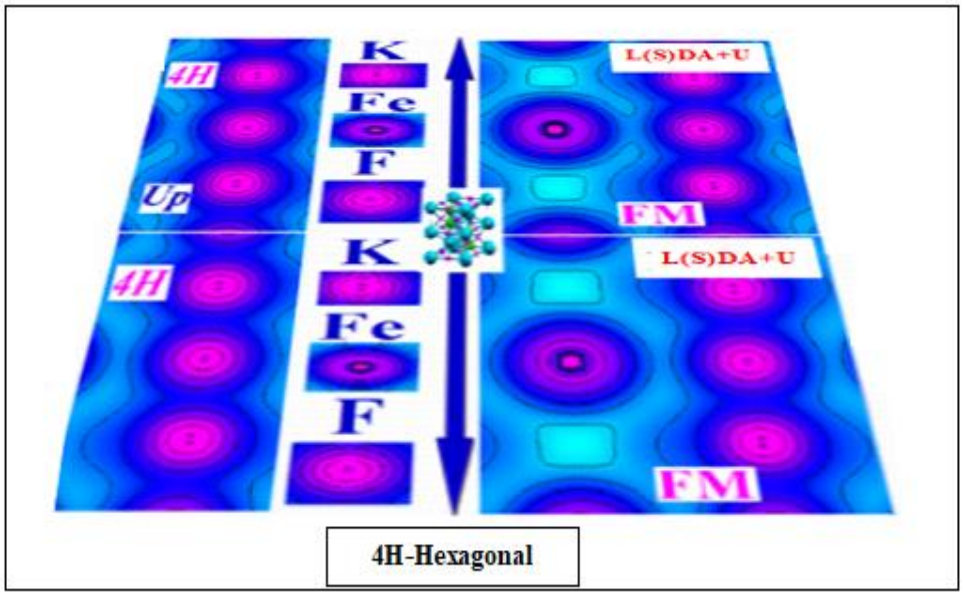

Figure 6b. Charge Densities for the 4H-Hexagonal (P6/mmc) phase $KFeF_3$ Fluoride with (L(S)DA+U) approach.

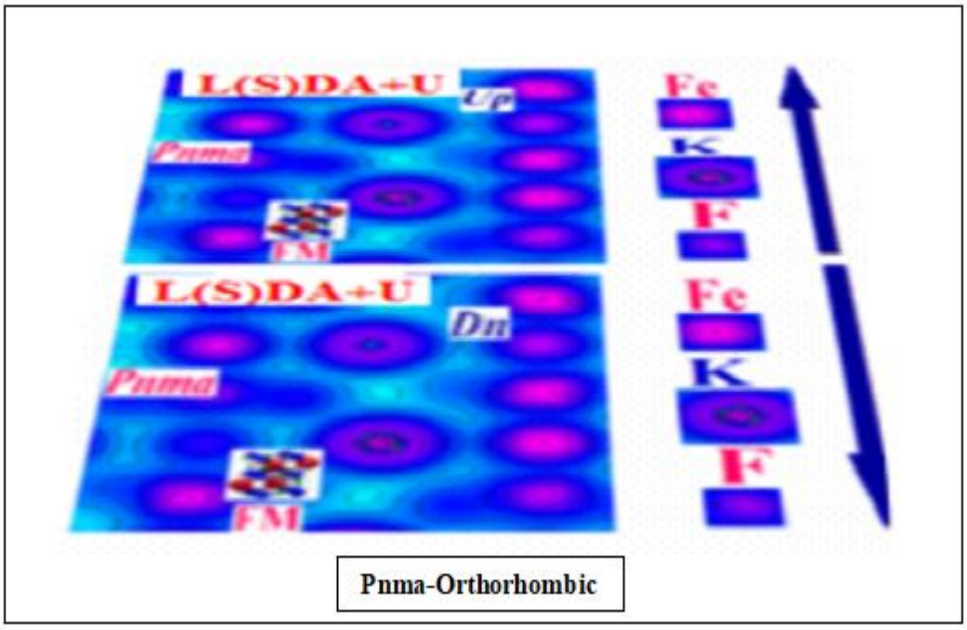

Figure 6c. Charge Densities for the Orthorhombic (Pnma) phase $KFeF_3$ Fluoride with (L(S)DA+U) approach.

5. Conclusion

To summarize, this comparative study of cation effect on the Fluorides $KFeF_3$, $KCoF_3$ and $KNiF_3$ investigated to show their electro-magnetic character in the cubic (Pm-3m), 4H (P6/mmc) and Orthorhombic (Pnma) phases and to give the systematic comprehension on these derivatives are given by L(S)DA and L(S)DA+U which is one of the mostly implemented methods in the DFT+U in order to show the stability phases between all phases

investigated here and compared with others works. Magnetic moment and spin effect is taken in consideration on the ground states properties of these Fluorides. The spin change in FM configuration between *3d* (Spin Up and Spin Dn-states), they will be well predicted by the Hubbard correction, while the pure DFT fails due to the correlation in the *d* orbitals of the centered transition-metal. In addition, the B-cation (Fe, Co, and Ni) modify enormously the nature of the transition by hybridizing with the valence state, transfer changes. The contribution of this cation is more dominant in comparison to the others especially Fluorine Fe. The current study shows that the Fluorides $KFeF_3$, $KCoF_3$ and $KNiF_3$ investigated here represent unique and special physical properties which allows them to be potential candidates in optoelectronic, spintronic, and Solar Cells devices.

References

[1] Hamdad Noura, Superlattices and Microstructures 76, 425 (2014).

[2] Noura, Hamdad, Physica B 406, 1194 (2011).

[3] Labdelli Abbes, Hamdad Noura, Results in Physics, 5, 38 (2015).

[4] Ravinder Kour, Sandeep Arya, Sonali Verma, Jyoti Gupta, Pankaj Bandhoria, Vishal Bharti, Ram Datt, and Vinay Gupta, Global Challenges, 3, 1900050 (2019).

[5] H. Tanaka, M. Misono, Curr. Opin. Solid State Mater. Sci., 5, 381, (2001).

[6] Wei Li, Run Long, Jianfeng Tang, and Oleg V. Prezhdo, J. Phys. Chem. Lett. 10, 3788, (2019).

[7] A. A. Mubarak, Journal of Electronic Materials, 47, 887 (2018).

[8] N. L. Allan, D. T. Kulp, W. C. Mackrodt, Journal of Fluorine Chemistry, 45, 186 (1989).

[9] Monique Body, Gilles Silly, Christophe Legein, Jean-Yves Buzaré, The Journal of Physical Chemistry B 20, 10270 (2005).

[10] David P. Dobson, Simon A. Hunt, Alexander Lindsay-Scott, Ian G. Wood, Physics of the Earth and Planetary Interiors, 189, 171 (2011).

[11] Saswata Dasgupta, Bhaskar Rana, John M. Herbert, J. Phys. Chem. B 38, 8074 (2019).

[12] Rune Søndenå, Svein Stølen, and P. Ravindran, Phys. Rev. B 75, 184105 (2007).

[13] J. L. Sommerdijk, A. Bril, Journal of Luminescence 11, 363 (1976).

[14] M. W. Shafer, Materials Research Bulletin, 4, 905 (1969).

[15] A. A. Mubarak, and A. A. Mousa, Comput. Mater. Sci. 59, 6 (2012).

[16] A. A. Mubarak, and Saleh Al-Omeri, Journal of Magnetism and Magnetic Materials 382, 211 (2015)

[17] Randal J. J., Ward R. J. Am. Chem. Soc. 81, 2629, (1959).

[18] K. Knox, Acta Cryst. 14, 583 (1961).

[19] Clément Jakymiw, Lidunka Vočadlo, David P. Dobson, Edward Bailey, Andrew R. Thomson, John P. Brodholt, Ian G. Wood, and Alex Lindsay-Scott, Phys Chem Miner. 4, 311 (2018).

[20] T. Nakajima, B. Žemva et A. Tressaud, Advanced Inorganic Fluorides: Synthesis, Characterization and Applications (2000).

[21] Eva Gil-GonzálezAntonio PerejónPedro E. Sánchez-JiménezJosé M. CriadoLuis *A.* Pérez-Maqueda, in Handbook of Thermal Analysis and Calorimetry, (2018).

[22] Ewa Kurzeja, Agnieszka Synowiec-Wojtarowicz, Małgorzata Stec, Marek Glinka, Stanisław Gawron, and Katarzyna Pawłowska-Góral, Int J Mol Sci. 7,15017, (2013).

[23] Ruren Xu , Wenquin Pang, and Qisheng Hu, Modern Inorganic Synthetic Chemistry (2010).

[24] Japanese Journal of Applied Physics 4A, 41 (2002).

[25] L. Grigorjevaa, D. K. Millersa, V. Pankratova, R. T. Williamsb, R. I. Eglitisc, E. A. Kotomina, d, G. Borstel, Solid State Communications 129, 691 (2004).

[26] K. Ephraim Babu, A. Veeraiah, D. Tirupati Swamy, V. Veeraiah, Chin. Phys. Lett. 29, 117102, (2012).

[27] Eva Gil-GonzálezAntonio PerejónPedro E. Sánchez-JiménezJosé M. CriadoLuis *A. Pérez-Maqueda, in* Handbook of Thermal Analysis and Calorimetry, *(2018).*

[28] G. Calestani, F. Mezzadri, *in* Photonic and Electronic Properties of Fluoride Materials, (2016).

[29] Alain Tressaud, in Fluorine, Fluorine, a key element for the 21st century, (2019).

[30] A. S. Verma, 158, 34, (2013).

[31] Konrad T. Semrau, Journal of the Air Pollution Control Association, (2012).

[32] P. Fazekas, Lecture Notes on Electron Correlations and Magnetism (World Scientific, Singapore), (1999).

[33] Jihara S. (2018) Sol-Gel Processing of Fluoride and Oxyfluoride Materials. In: Klein L., Aparicio M., Jitianu A. (eds) Handbook of Sol-Gel Science and Technology. Springer, Cham, 1, 27 (2017).

[34] Stepan Syrotyuk, Solid State Phenomena 230, 79 (2015).

[35] Richard D. Chambers FRS, Fluorine in Organic Chemistry, (2004).

[36] C. F. Matta and R. J. Gillespie, Journal of Chemical Education, 79, 1141, (2002).

[37] P. Fazekas, Lecture Notes on Electron Correlations and Magnetism, World Scientific, Singapore, (1999).

[38] M. Imada, A. Fujimori, Y. Tokura, Rev. Mod. Phys. 70, 1039 (1998).

[39] S. Yamada, N. Abe, H. Sagayama, K. Ogawa, T. Yamagami, T. Arima, Phys. Rev. Lett. 123, 126602 (2019).

[40] Nadeem Hussain, Fangfang Wu, Waqar Younas and Liqiang Xu, New J. Chem., 43, 11959 (2019).

[41] Qianjin Zhu, Jihuai Wu, Pengqiang Yuan, Mingjing Zhang, Yanfei Dou, Xiaobing Wang, Jinjun Zou, Weihai Sun, Leqing Fan, and Zhang Lan, Energy Technology, 8, 1901017, (2020).

[42] Nengxu Li, Shuxia Tao, Yihua Chen, Xiuxiu Niu, Chidozie K. Onwudinanti, Chen Hu, Zhiwen Qiu, Ziqi Xu, Guanhaojie Zheng, Ligang Wang, Yu Zhang, Liang Li, Huifen Liu, Yingzhuo Lun, Jiawang Hong, Xueyun Wang, Yuquan Liu, Haipeng Xie, Yongli Gao, Yang Bai, Shihe Yang, Geert Brocks, Qi Chen and Huanping Zhou, Nature Energy, 4, 408 (2019). [43] Zhou, H. et al. Interface engineering of highly efficient perovskite solar cells. *Science* 345, 542, (2014).

[44] J. P. Perdew and K. Burke, Int. J. Quantum Chem. 57, 309 (1996).

[45] F. Tran and P. Blaha, Phys Rev. Lett. 102, 226401 (2009)

[46] P. Blaha, K. Schwarz, G. K. H. Madsen, D. Kvasnicka and J. Luitz, WIEN2k, K. Schwarz, Techn. University at Wien, Austria, 3, 9501031 (2001).

[47] P. Hohenberg and W. Kohn, Phys. Rev. B 136, 864 (1964).

[48] W. Kohn and L. J. Sham, Phys. Rev. 140, A1133 (1965).

[49] J. P. Perdew, S. Burke and M. Ernzerhof, Phys. Rev. Lett. 77,3865 (1996).

[50] Tanghong Yi, Wei Chen, Lei Cheng, Ryan D. Bayliss, Feng Lin, Michael R. Plews, Dennis Nordlund, Marca M. Doeff, Kristin A. Persson, and Jordi Cabana, Investigating the Intercalation Chemistry of Alkali Ions in Fluoride Perovskites, 10.1021/acs.chemma-536ter.6b04181.

[51] Pena, M. A.; Fierro, J. L. G. Chemical Structures and 678 Performance of Perovskite Oxides. Chem. Rev. 101, 1981 (2001).

[52] Goldschmidt, V. V. M Die Gesetze der Krystallochemie. 680 Naturwissenschaften, 14 477, (1926).

[53] Jaeryeong Lee, Heeyoung Shin1, Jaechun Lee1, Hunsaeng Chung1, Qiwu Zhang and Fumio Saito, Materials Transactions, 44, 1457 (2003).

[54] V Manivannan, P Parhi and Jonathon W Kramer, Bull. Mater. Sci., 31, 987 (2008).

[55] Lee J, Zhang Q and Saito F, Chem. Lett. 7, 700 (2001).

[56] Lee J, Shin H, Lee J, Chung H, Zhang Q and Saito F Mater. Trans. 44, 1457, (2003).

[57] Atsushi Okazaki, Yasutaka Suemune, Journal of the Physical Society of Japan, 16, 671 (1961).

[58] Mats Johnsson and Peter Lemmens, Crystallography and Chemistry of Perovskites, (2007).

[59] M.M. J. Portier, A. Tressaud, J-L. Dupin et R. de Pape., Mat. Res. Bull. 4, 45, (1969).

[60] K. Knox, Acta Cryst. 14, 583, (1961)

[61] R. Fatehally, G. K. Shenoy, N. P. Sastry and R. Nagarajan, Phys. Lett. 25A, 454, (1967)

[62] E. N. Maslen, N. Spaldaccini, T. Ito, F. Marumo, K. Tanaka, Y. Satow, Acta Crystall. B 49, 632 (1993).

[63] Munetaka Haida, and Kay Kohn, Journal of the Physical Society of Japan 40, 981 (1976).

[64] M. Safa and B. K. Tanner, B. J. Garrard and B. M. Wanklyn, J. Crystal Growth 39, 243 (1977).

[65] M. P. J. Punkkinen, Solid State Communications 111, 477(1999).

[66] A. S. Verma, Solid State Communications 158, 34, (2013).

[67] F. S. Galasso, Perovskites and High Tc Superconductors, Wiley, NewYork, (1990).

[68] M. Kestigian, F. D. Leipziger, W. J. Croft et R. Guidoboni, Inorg. Chem. 5, 1462, (1966).

[69] O. Muller, R. Roy, The Major Ternary Structural Families, Springer, New York, (1974).

[70] Liu Liang, Lu Wencong, Chen Niany, Journal of Physics and Chemistry of Solids 65, 855 (2004)

[71] A. S. Verma, Solid State Communications, 158, 34 (2013).

[72] A. S. Verma, A. Kumar and S. R. Bhardwaj, Physica Status Solidi B 245, 1520 (2008).

[73] A. S. Verma and A. Kumar, J. Alloys and Compounds, 541, 210 (2012).

[74] A. S. Verma and V. K. Jindal, J. Alloys and Compounds, 485, 514 (2012).

[75] Joanna Kapusta, Philippe Daniel, and Alicja Ratuszna, Phys. Rev. B59, 14235 (1999).

[76] Alicja Ratuszna, Joanna Kapusta, Phase Transitions 62, 181 (1997).

[77] Kunio Saiki. Resonance behaviour in canted antiferromagnet $KMnF_3$. Journal of the Physical Society of Japan, 33, 1284 (1972).

[78] P. S. Whitfield, N. Herron, W. E. Guise, K. Page, Y. Q. Cheng, I. Milas & M. K. Crawford, Scientific Reports, 6, 35685 (2016).

[79]: Madan Lal and Shikha Kapila, International Journal of Materials Science 12, 137 (2017).

[80] Ruinian Hua, Zhihong Jia, Demin Xie, Chunshan Shi, Chemistry Letters, 31, 538 (2002).

[81] Andréa Martin, Enrique S. Santiago, Erhard Kemnitz, and Nicola Pinna, ACS Appl. Mater. Interfaces, 11, 33132 (2019).

[82] J. Ferré, B. Briat, R.H. Petit, R.V. Pisarev et J. Nouet, J. Phys. France, 5, 503 (1976).

[83] A.Oleaga, A.Salazar, D.Skrzypek, Journal of Alloys and Compounds, 629, 178 (2015).

[84] S.L. Wang, W. L. Li, G. F. Wang, D.Y. Dong, J. J. Shi, X. Y. Li, P.G. Li, and W. H. Tang, Crystal structure and Electrical transport property of KMF_3 (M= Mn, Co and Ni), Cambridge University Press.

[85] R. Dovesi, F. Fava, F. C. Roetti and V. R. Saunders, Faraday Discuss 18, 569 (1997)

[86] O.Beckman and K. Knox, Phys. Rev, 121, 376 (1961).

[87] S. A. Kizhaev, and Markova, Phys. Solid State 53, 1851 (2011).

[88] G. F. Du, J. Zuo, and O. Yang, Chin, J. Chem. Phys. 18, 569 (2005).

[89] E. K. H Sajle, M. Zhang, and H. Zhang, J. Phys. Condens Matter 21, 33 (2009).

[90] A. J. Heeger, O. Beckman, and A. M. Portis, Phys. Rev. B 25, 3538 (1961).

[91] F. D. Murnaghan, Proc. Natl. Acad. Sci. USA, 30, 5390 (1944).

[92] Karlheinz Schwar, Peter Blaha, and S.B. Trickey, Molecular Physics 108, 21 (2019).

[93] Blaha, P., Schwarz, K., Sorantin, and P. & Trickey, Comput. Phys. Commun. 59, 399 (1990).

[94] Georg K. H. Madsen, Peter Blaha, Karlheinz Schwarz, and Lars Nordström, Physical Review B 64, 19, (2001).

[95] The DFT+U: Approaches, Accuracy, and Applications, Open access peer-reviewed chapter, Sarah A. Tolba, Kareem M. Gameel, Basant A. Ali, Hossam A. Almossalami and Nageh K. Allam (2018).

[96] Peter Blaha, Karlheinz Schwarz, Georg K. H. Madsen, Dieter Kvasnicka, Joachim Luitz, Robert Laskowski, Fabien Tran, and Laurence D. Marks, User's Guide, WIEN2k (2019).

[97] Burak Himmetoglu , Andrea Floris , Stefano de Gironcoli and Matteo Cococcioni, Quantum Chemistry, 114, 14, (2014).

[98] M. *Cococcioni* and S. de Gironcoli, PRB 71, 035105 (2005).

[99] H. J. Monkhorst, J. D. Pack, Phys. Rev. B 13, 5192 (1976).

[100] G. Vaitheeswaran, V. Kanchana, R.S. Kumar, A.L. Cornelius, M.F. Nicol, A. Svane, A. Delin, B. Johansson, Phys. Rev. B 76, 014107 (2007).

[101] Hayatullah, G. Murtaza, R. Khenata, S. Naeem, M.N. Khalid, S. Mohammad, Chin. Phys. Lett. 30, 097101 (2013).

[102] G. Pari, S. Mathi Jaya, and R. AsokamaniPhys. Rev. B 50, 8166 (1994).

[103] Rune Søndenå, Svein Stølen, and P. Ravindran, Tor Grande, Neil L. Allan, Phys. Rev. B 75, 184105 (2007).

[104] Rune Søndenå, P. Ravindran, Svein Stølen, Tor Grande, Michael Hanfland,Electronic structure and magnetic properties of cubic and hexagonal SrMnO3,Phys. Rev. B 74 (2006) 144102.

[105] Dimov, N.; Nishimura, A.; Chihara, K.; Kitajou, A.; Gocheva, I. D.; Okada, S. Transition Metal $NaMF_3$ Compounds as Model Systems (2013).

[106] Chaplygin I, Seifert G, Gemming S, Laskowski R. Comput Mater Sci 44, 79, (2008).

[108] C. Cros, R. Feurer et M. Poucliard, J. Fluorinr Chem., 7, 605 (1976).

[109] Roberto L. Moreiraa, and Anderson Dias; Comment on "Prediction of lattice constant in cubic perovskites, J. Phys. Chem. Solids 67, 1531 (2006).

[110] Huggins, R. A. & Rabenau, S. Mater. Res. Bull. 13, 1315, (1978).

[111] Hayatullah, G. Murtaza R. Khenata, S. Muhammada, A. H. Reshak, Kin Mun Wongf, S. Bin Omran , Z. A. Alahmed, Computational Materials Science 85, 402 (2014).

[112] M. Abdul, S. L. Yeon, Adv. Inf. Sci. Serv. Sci. 2, 3 (2010).

[113] J. Silver, Journal of Fluorine Chemistry, 8, 527 (1976).

[114] A. Okazaki, Y. Suemune, T. Fuchikami, J. Phys. Soc. Jpn 14, 1823 (1959).